International Journal of Biological Macromolecules 321 (2025) 146497

Contents lists available at ScienceDirect

International Journal of Biological Macromolecules

journal homepage: www.elsevier.com/locate/ijbiomac

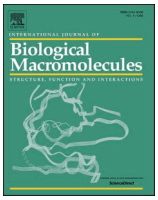

Extraction and characterization of lignin from lignocellulose biomass using citric acid and fructose-based NADES

Mohsin Raza [a,b], Arafat Husain [a], Mohammad Jawaid [a], Abrar Inayat [c], Yaser E. Greish [d], Aatikah Meraj [e], Basim Abu-Jdayil [a,*]

[a] Chemical and Petroleum Engineering Department, College of Engineering, United Arab Emirates University, 15551 Al Ain, United Arab Emirates
[b] Research Institute of Science and Engineering, Biomass and Bioenergy RG, University of Sharjah, 27272 Sharjah, United Arab Emirates
[c] Department of Mechanical and Nuclear Engineering, University of Sharjah, 27272 Sharjah, United Arab Emirates
[d] Department of Chemistry, United Arab Emirates University, Al Ain, 15551, Abu Dhabi, United Arab Emirates
[e] Laboratory of Bio-polymer and its Derivatives, Institute of Tropical Forestry and Forest Products (INTROP) University Putra Malaysia UPM, 43400 Serdang, Selangor, Malaysia

ARTICLE INFO

Keywords:
Lignin Extraction
Natural Deep Eutectic Solvent
Fruit-based NADES
Biomass fractionation
Green Chemistry

ABSTRACT

Lignin, an important biopolymer in lignocellulosic biomass, is key to sustainable material applications and advances in biorefinery. Over the past decade, deep eutectic solvents (DES) have appeared as environmentally friendly solvents for lignin extraction, with choline chloride-based DES being widely used. Choline chloride, though biodegradable, is synthesized using hydrochloric acid, making it not fully organic. In this study, a 100 % organic, natural deep eutectic fruit-based solvent (NADES) composed of citric acid and fructose was used for the first time for lignin extraction. An acid-free lignin recovery protocol was also developed, eliminating the need for the traditional acid precipitation method and bringing the entire process in line with green chemistry principles. NADES were produced at different molar ratios and pH values to optimize the lignin dissolution. At pH 1.4, a maximum yield of 9.50 % by weight and a recovery rate of 44.10 % were achieved. Scanning electron microscopy and elemental analysis confirmed the removal of non-lignin components, whereas ultraviolet spectroscopy, Fourier transform infrared spectroscopy, and X-ray diffraction confirmed the enrichment of lignin. The aromatic structure of lignin was preserved, ensuring high purity and no degradation of the aromatic structure. Thermogravimetric and differential scanning calorimetry analyses showed the thermal stability of the extracted lignin, while the activation energy (E_a) and elemental analysis indicated carbon enrichment. In this study, a novel lignin extraction method using 100 % organic fruit-based NADES combined with an acid-free recovery process is presented, which represents a significant advancement in this field.

1. Introduction

Research on the development of sustainable and renewable technologies with a main focus on maximum utilization of green technologies is crucial to meet the United Nations Sustainability Goals [1]. Lignocellulosic biomass is an economical, renewable, and sustainable resource with a vast potential for bioenergy production and the development of biomaterials [2]. It primarily consists of three essential biopolymers: lignin (20–25 %), cellulose (45–50 %), and hemicellulose (20–25 %) [3]. Lignin, which acts as the "glue" binding cellulose and hemicellulose, is water-insoluble and highly stable [4]. As the second most abundant polymer after cellulose, approximately 3×10^{11} metric tons of lignin exists globally, with an annual biosynthesis of approximately 2×10^{11} metric tons [5]. Owing to its rich aromatic structure, lignin is widely used in the production of biofuels, bioplastics, and carbon fibers while also serving as a sustainable alternative to petroleum-based chemicals in adhesives, coatings, and polymer composites [6].

The lignocellulose structural matrix is a complex network in which cellulose is encapsulated by a hemicellulose monolayer and embedded within a core matrix of lignin and hemicellulose, making component separation challenging [7]. Conventional fractionation processes rely on toxic chemicals like sodium hydroxide, sodium chlorite, and sodium hypochlorite, used at high concentrations (8–10 %) at elevated

* Corresponding author.
E-mail address: babujdayil@uaeu.ac.ae (B. Abu-Jdayil).

https://doi.org/10.1016/j.ijbiomac.2025.146497
Received 7 May 2025; Received in revised form 16 July 2025; Accepted 31 July 2025
Available online 5 August 2025

temperatures (80–100 °C) [8]. While effective, these methods require pre-treatment before discharge to mitigate environmental damage, posing significant sustainability concerns [9]. The use of green solvents to fractionate lignocellulosic biomass holds significant promise as a sustainable and environmentally friendly alternative to conventional chemical methods [10].

Natural deep eutectic solvents (NADES) are regarded as solvents of the 21st century because of their eco-friendly and cost-effective nature [11]. Composed of two inexpensive, renewable, and biodegradable components, they serve as sustainable alternatives to conventional solvents, effectively fractionating biomass into lignin and cellulose streams [12]. NADES are mostly made by combining choline chloride with organic acids, such as formic, acetic, or citric acid, and are easy to produce and have low toxicity [13]. One of the most important advantages is the recovery of NADES after the pre-treatment process [14]. Chen et al. [15] conducted a review and found that over 30 studies on lignin extraction from lignocellulosic biomass have involved the use of choline chloride-based NADES. Similarly, Xiao et al. [16], in their review of lignocellulose fractionation using NADES, also reported the dominance of choline chloride-based NADES for lignin dissolution. Choline chloride is widely used in NADES production owing to its advantageous properties. Choline chloride is a synthetic compound formed by combining choline (a natural nutrient) with hydrochloric acid [17]. Therefore, it is biodegradable and low in toxicity but is not considered fully organic because of its chemical synthesis. NADES have also been used in the extraction of other natural compounds such as alkaloids [18], triterpene saponins [19], polysaccharides [20], glycosides and aglycones of phenyletanes, phenylpropanoids [21], curcumins [22], steviol glycosides [23], epoxysesquiterpene [24], essential oils [25], steroidal saponins [26], as well as specialized metabolites [27].

Lignin collection is an important step once a lignin is extracted from lignocellulosic biomass. The common practice involves lowering the pH, typically by adding an acid such as sulfuric acid, which causes lignin to solidify and separate [28]. In a study by Meraj et al. [29], lignin was extracted from NADES-pretreated kenaf fiber biomass. NADES were prepared using choline chloride and lactic acid in a 2:1 M ratio. Lignin precipitation was achieved using 72 % sulfuric acid hydrolysis. The sulfuric acid precipitation of lignin has several disadvantages, including its environmental impact due to the generation of sulfate-containing waste, which requires careful disposal to avoid pollution [30]. In the study by Sharma et al. [31], acetic acid and lactic acid as precipitation solvents for lignin from kraft black liquor. This substitution was motivated by concerns regarding the environmental and process safety associated with sulfuric acid.

The Ghaf tree *(Prosopis cineraria)*, declared the national tree of the UAE, has great cultural and environmental significance [32]. Its deep root system allows it to thrive in a harsh desert climate by accessing groundwater far below the surface, making it a vital species for maintaining ecological balance in arid regions. As a result, the cultivation of Ghaf trees has been steadily increasing in the UAE and MENA, playing a crucial role in regional afforestation. However, the cultivation process generates significant waste, particularly lignocellulosic biomass waste [33].

The study aimed to extract lignin using a completely green solvent rather than commonly used choline-chloride-based NADES. Therefore, this serves as the first study to use 100 % organic fruit-based NADES for lignin extraction, combined with an acid-free protocol to obtain lignin, making the entire process environmentally safe. The freeze-drying and subsequent drying in an oven eliminates the need for using conventional acid-containing protocols for lignin collection. The purity, physiochemical, and thermal characteristics of the extracted lignin were analyzed using advanced characterization techniques, including scanning electron microscopy, energy-dispersive X-ray spectroscopy, ultraviolet-visible spectroscopy, X-ray diffraction, Fourier transforms infrared spectroscopy, thermogravimetric analysis, differential scanning calorimetry, and elemental analysis.

2. Materials and methods

2.1. Materials

Ghaf waste biomass was obtained from agricultural farms. The collected biomass was shredded and ground to pass through a sieve size of 120 μm. Citric acid ≥99.5 % (CA: CAS 77–92-9) and fructose ≥99 % (Fr: CAS 57–48-7) were obtained from Sigma-Aldrich and used without any modification.

2.2. Preparation of Natural Deep Eutectic Solvent (NADES)

CA/Fr NADES were prepared using a conventional heating and stirring method. CA and Fr were mixed at a fixed molar ratio, and 1 mL of distilled water (DI) was added to reduce the initial viscosity, becoming part of the NADES superstructure. The mixture was stirred at 600 rpm for 10 min in a flask to ensure optimal mixing. Once stirring was complete, the mixture was heated to 100 °C to evaporate the DI. After the water had completely evaporated, the resulting yellowish NADES were obtained. Prior to biomass treatment, a fixed volume/volume (*v*/v) dilution ratio of 3:1 (i.e., 3 mL water to 1 mL NADES) was used to lower the viscosity and enhance diffusion into the lignocellulosic matrix. The nomenclature for the NADES mixtures was based on the molar ratio of CA, Fr, and DI, with a dilution ratio of volume/volume (3 *v*/v). Table 1 shows the molar ratio and pH of the NADES.

A stable NADES is formed due to hydrogen bonding between hydroxyl groups of fructose and carboxylic groups in citric acid. In this system, citric acid acts as a hydrogen bond donor and fructose acts as a hydrogen bond acceptor. The variation in the molar ratio of citric acid and fructose results in changes in the hydrogen bond density and acidity of NADES. This influenced lignin solubility.

The addition of water affects the properties and performance of NADES. It influences the main properties, such as density, refractive index, and pH, which are important for the application of NADES [34]. In this study, a fixed dilution ratio of 3:1 (v/v, water: NADES) was used to reduce viscosity while conserving the eutectic structure. If water was not added to dilute the NADES, the highly viscous solvent was not easily favorable for the processability of lignocellulose biomass treatment. However, comparison studies in the future can be performed to investigate the performance of CA/FR NADES for lignin extraction with and without the addition of water. Other authors have fractionated lignocellulose biomass wastes using choline chloride-based NADES. Liu et al. [35] have fractionated lignocellulose biomass using NADES consisting of choline chloride and oxalic acid in a molar ratio of ChCl: OA = 1:1. Salcido et al. [36] treated lignocellulose biomass using NADES consisted of choline chloride and lactic acid in a molar ratio of ChCl: LA = 1:9.

2.3. Lignin extraction

The Ghaf waste was treated with NADES at a biomass-to-solvent ratio (*w*/*v*) of 1:10. The mixture was stirred at 500 rpm, maintained at 60 °C for 3 h., and the reaction was terminated by adding 20 mL of cold water (4 °C). The mixture was vacuum-filtered to obtain a lignin-NADES suspension as the filtration. The lignin-NADES suspension was lyophilized using a Labtron LBFD-D11 freeze dryer at −85 °C, 0.001 mPa for 24 h. The purpose of freezing was to preserve the structural integrity and avoid thermal degradation of the extracted lignin, mainly its functional groups and aromatic structures. Freeze-drying ensures mild elimination

Table 1
Composition and pH of NADES.

NADES	Molar ratio	Dilution water (mL/1 mL of NADES)	pH
CA/Fr/DI	1:1:1	3	1.70
CA/Fr/DI	3:1:1	3	1.54
CA/Fr/DI	5:1:1	3	1.40

of moisture and the residual NADES from lignin under low temperature and vacuum conditions, thereby avoiding possible changes in the lignin's physicochemical properties.

The thick paste containing lignin and residual NADES was then mixed with 20 mL of fresh deionized water (DI) and dried in an air-circulating oven at 105 °C for 24 h. The lignin was further stirred with 20 mL of DI for 5 mins, and the drying process was repeated three times until fully dry dispersible lignin particles were obtained.

Because the NADES components (fructose and citric acid) have boiling points higher than 105 °C, they cannot evaporate directly at this temperature. However, dissolving lignin and residual NADES in water disrupts the eutectic structure, effectively lowering the NADES boiling point. This promoted co-evaporation, where water vapor carried away residual NADES components during drying at 105 °C. Repeated washing and drying cycles ensured the complete removal of pure, dispersible lignin particles. Fig. 1 presents an overview of the complete extraction process.

2.4. Characterization methods

2.4.1. Yield and chemical composition

The chemical composition was determined using standard ASTM (D1104–56, D1103–60, D1104–56) and TAPPI (T 204 cm-97) protocols. Details of the procedures are available in our previous publications [37]. The yield of lignin extracted from the Ghaf biomass waste was determined using Eq. 1 [38]:

$$\textbf{\textit{Yiled}} = \frac{\textbf{\textit{Extracted Lignin (Dried)}}}{\textbf{\textit{Inital Ghaf Biomass Waste}}} \quad (1)$$

2.4.2. SEM and EDX analysis

The elemental composition and morphological characteristics of the Raw Ghaf Waste and Extracted Lignin were analyzed using energy dispersive X-ray spectroscopy (EDX) and scanning electron microscopy (SEM) with a JEOL JSM-6390 A (Japan). To mitigate electrostatic charging during imaging, the samples were coated with a thin layer of gold and tests were performed under a N_2 atmosphere.

2.4.3. UV–Vis spectroscopy

A UV–Vis spectroscopy analyzer (Spectrostar Nano, BMG LABTECH) was used to analyze the extracted lignin in the range of 20–800 nm. The extracted lignin was dispersed in a 0.1 M NaOH solution and sonicated for 10 min before analysis.

2.4.4. XRD analysis

Structural analysis of Raw Ghaf Waste and Extracted Lignin was conducted using Cu Kα radiation under operating parameters of 40 kV, 30 mA, and a receiving slit width of 0.15 mm. Diffraction intensity measurements were recorded over a scan range of 10–80° at a scanning speed of 2°/min. The crystallinity indices of the samples were calculated using the Segal equation, as shown in Eq. 2 [39].

$$\boldsymbol{C_{rl}} = \frac{I_{200} - I_{am}}{I_{200}} \quad (2)$$

Where I_{200} is the intensity of the crystalline peak and I_{am} is the intensity of the amorphous peak.

2.4.5. FTIR analysis

A Fourier-transform infrared (FTIR) spectrometer (Shimadzu, Kyoto, Japan) was used to analyze the functional groups present in the Raw Ghaf Waste and Extracted Lignin. Infrared spectra were recorded using an attenuated total reflectance (ATR) accessory, covering a wavelength range of 400–4000 cm^{-1}. The measurements were conducted using 34 scans at a spectral resolution of 4 cm^{-1}.

2.4.6. TGA analysis

Thermogravimetric analysis (TGA) was performed on the Raw Ghaf Waste and Extracted Lignin using a Q500 series analyzer (TA Instruments, USA) with a sample weight range of 5–10 mg. The thermal decomposition behavior of both samples was evaluated under non-isothermal conditions in a nitrogen atmosphere at a flow rate of 60 mL/min. A uniform heating rate of 10 °C/min was applied, starting at 25 °C and increasing up to 700 °C.

2.4.7. DSC analysis

The thermal transition behavior of the extracted lignin was examined using differential scanning calorimetry (DSC) with a DSC25 instrument (TA Instruments, USA). Sample weights ranging from 5 mg to 10 mg were analyzed under a nitrogen atmosphere at a flow rate of 50 mL/min. The temperature increased from 30 °C to 300 °C at a controlled heating rate of 10 °C/min.

2.4.8. E_a analysis

The activation energy (E_a) values, based on experimental TGA data at specified heating rates β (5, 10, and 15 °C/min), were determined using model-free methods, such as FWO, KAS, and STK, as described by Fu et al. [40], Wang et al. [41], and Mai et al. [42]. These methods are mathematically expressed in (Eqs. (3)–(5)):

$$\textbf{FWO}: \quad \ln(\beta) = \ln\left(\frac{A \times E_a}{R \times g(\alpha)}\right) - 5.331 - 1.052\left(\frac{E_a}{RT}\right), \quad (3)$$

$$\textbf{KAS model}: \quad \ln\left(\frac{\beta}{T^2}\right) = \ln\left(\frac{A \times R}{E_a \times g(\alpha)}\right) - \frac{E_a}{RT}, \text{ and} \quad (4)$$

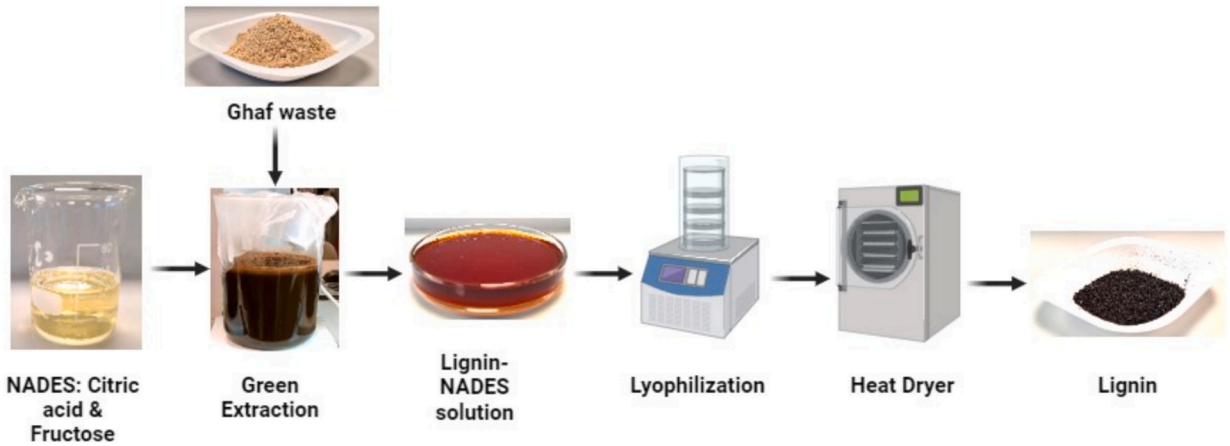

Fig. 1. An Overview of Lignin Extraction from Ghaf waste using NADES.

STK :
$$\ln\left(\frac{\beta}{T^{1.92}}\right) = C_s - 1.008\left(\frac{E_a}{RT}\right). \quad (5)$$

In the FWO method, ln(β) is plotted against 1/T, and the resulting slope is 1.052 E_a/R. Similarly, plotting ln(β/T^2) versus 1/T in the KAS method yields a linear relationship with a slope equal E_a. In the STK method, linear regression of ln(β/$T^{1.92}$) versus 1/T yields E_a.

2.4.9. Elemental analysis

Ultimate analysis was conducted using a CHNS/O elemental analyzer to determine the weight percentages of carbon, hydrogen, nitrogen, sulfur, and oxygen in the raw Ghaf waste and extracted lignin.

3. Results and discussion

3.1. Yield and chemical composition

Raw Ghaf waste contained 45.30 ± 1.50 wt% cellulose, 33.33 ± 1.50 wt% hemicellulose and 21.50 ± 2.40 wt% lignin. The relatively high standard deviation observed in the lignin content could be due to the mass losses that occur during processes such as vacuum filtration, freeze-drying, and evaporation. Table 2 shows that increasing the molar ratio of citric acid (CA) in NADES steadily decreased the pH, producing acidic conditions that significantly improved lignin dissolution. When the pH drops from 1.70 to 1.40, the lignin yield increases significantly from 5.55 ± 0.15 to 9.50 ± 0.20 wt% and the recovery from 25.80 ± 2.96 to 44.10 ± 5.01 wt%. The acidic NADES composition, with a pH value of 1.40, exhibits the highest efficiency in lignin extraction and recovery, as it effectively breaks up the complex polymer structure of lignin and thus significantly increases its solubility. In this study, the lignin extracted at the lowest pH and highest recovery was further analyzed for characterization. Other authors have used NADES, mainly composed of choline chloride. Owhe et al. [43] extracted lignin with a yield of 19.90 % from rick husk biomass using a NADES consisting of choline chloride and formic acid (ChCl: FA = 1:2). Lynam et al. [44] extracted lignin from loblolly pine biomass with a mass solubility of 12 % using NADES consisted of choline chloride and acetic acid (ChCl: AC = 1:10). Provost et al. [45] extracted lignin from sawmill chips with a yield of 39.30 % using a NADES consisted of choline chloride and lactic acid (ChCl: LA = 1:10). Mankar et al. extracted lignin from coconut coir with a high yield of 82 % using NADES consisting of choline chloride and lactic acid (ChCl: LA = 1:4).

3.2. Scanning Electron Microscopy (SEM)

Fig. 2 shows SEM images of raw Ghaf waste (a-b) and extracted lignin (c-d) at two different magnifications. In the raw Ghaf waste, the surface was rough, fibrous, and porous, indicating the presence of tightly bound cellulose, hemicellulose, and lignin. Loose fiber aggregates, surface debris, and structural irregularities reflect the complex and heterogeneous nature of biomass. In contrast, the extracted lignin exhibited a smoother and more homogeneous surface with negligible fibers or pores, confirming the removal of polysaccharides. The absence of a fibrous network and reduced porosity validated the successful extraction of lignin. Some layering or fractures observed in the extracted lignin reflect its brittleness. Similarly, Zhu et al. [46] obtained clear and smooth lignin free from non-lignin fibers and voids. Morphological analysis confirmed the effectiveness of this two-step lignin extraction and non-precipitation method for successfully extracting and obtaining purified lignin from lignocellulosic waste.

Table 2
Yield and recovery of extracted lignin.

NADES composition	Molar ratio	pH	Yield (wt%)	Recovery (wt%)
CA/Fr/DI	1:1:1	1.70	5.55 ± 0.15	25.80 ± 2.96
CA/Fr/DI	3:1:1	1.54	7.83 ± 0.22	36.40 ± 4.19
CA/Fr/DI	5:1:1	1.40	9.50 ± 0.20	44.10 ± 5.01

3.3. Elemental analysis

Fig. 3 shows the Energy Dispersive X-ray (EDX) analysis of (a) raw Ghaf waste and (b) extracted lignin, highlighting the changes in the elemental composition. Table 3 provides a detailed summary of the elemental compositions of the samples. Peaks corresponding to carbon (C) are observed at 0.3 keV and 0.4 keV, while oxygen (O) peaks appear at 0.5 keV. In the raw Ghaf waste, the carbon content was 63.15 ± 2.02 mass%, which increased to 69.73 ± 0.54 mass% in the extracted lignin, representing an approximate increase of 10.42 %. This increase confirms the removal of non-carbonaceous components such as cellulose and hemicellulose, leaving behind lignin, a carbon-rich polymer [47]. Similarly, the oxygen content decreases from 35.10 ± 3.19 mass% in the raw Ghaf waste to 30.28 ± 0.54 mass% in the extracted lignin, indicating an approximately 13.74 % reduction. This reduction results from the elimination of oxygen-rich polysaccharides (cellulose and hemicellulose) and hydroxyl groups, thereby increasing the carbon-to-oxygen ratio of lignin. The EDX spectrum of the raw Ghaf waste also showed peaks for Na (1.0 keV), Mg (1.3 keV), and Al (1.5 keV), indicating the presence of inorganic minerals, which are native to the raw biomass. These peaks were absent from the extracted lignin, further confirming the removal of mineral impurities during the extraction process. Similarly, Intapun et al. [48] conducted an EDX analysis of lignin and reported carbon and oxygen weight percentages of 45.54 % and 54.46 %, respectively. EDX analysis confirmed the effectiveness of this two-step lignin extraction and non-precipitation method for successfully extracting and obtaining a lignin with a high carbon-to-oxygen ratio.

3.4. UV–Vis spectroscopy

UV–Vis spectroscopy is recognized as a simple, fast, and economical analytical method and is therefore widely used for both qualitative and quantitative analyses of lignin [49]. UV–Vis spectroscopy is a reliable method for assessing lignin purity, with strong absorbance in the 280–300 nm range, indicating aromatic content through π → π* transitions. A clear peak in this range, which is not disturbed by other peaks, indicates high purity and minimal contamination by non-lignin components [50].

Fig. 4 shows the UV–Vis spectrum of the extracted lignin sample, which exhibits a sharp absorption peak at 280 nm, characteristic of the electronic π → π* transitions in the aromatic rings of the phenylpropanoid units of lignin. This absorption behavior falls within the preferred range for lignin (280–300 nm), confirming a high concentration of aromatic structures. The absence of distinct peaks associated with carbohydrate or protein impurities indicated that the lignin sample had a high degree of purity. Therefore, the extracted lignin was of high quality, with a desirable aromatic content and minimal impurities. In addition, the spectrum showed a broad and persistent plateau between 300 and 500 nm, indicating the presence of condensed aromatic structures or cross-linked networks that may have resulted from the lignin extraction method. Meraj et al. [29] reported that lignin extracted from kenaf fibers exhibited absorption peaks only beyond 300 nm, indicating a shift in the UV–Vis spectrum and alterations in the aromatic ring structure within the polymer. However, in this study, 100 % organic fruit-based NADES exhibited spectra precisely at 280 nm, indicating that NADES did not alter the aromatic structure of lignin. This suggests that the NADES extraction method used in this study preserves the structural integrity of lignin without significant degradation or modification of its aromatic units. This also confirmed that no excessive oxidation, condensation, or structural breakdown occurred during the extraction process. The resulting high-purity lignin is particularly beneficial for applications that require structural integrity and chemical functionality, such as the production of bio-based resins, carbon fibers, and adhesives

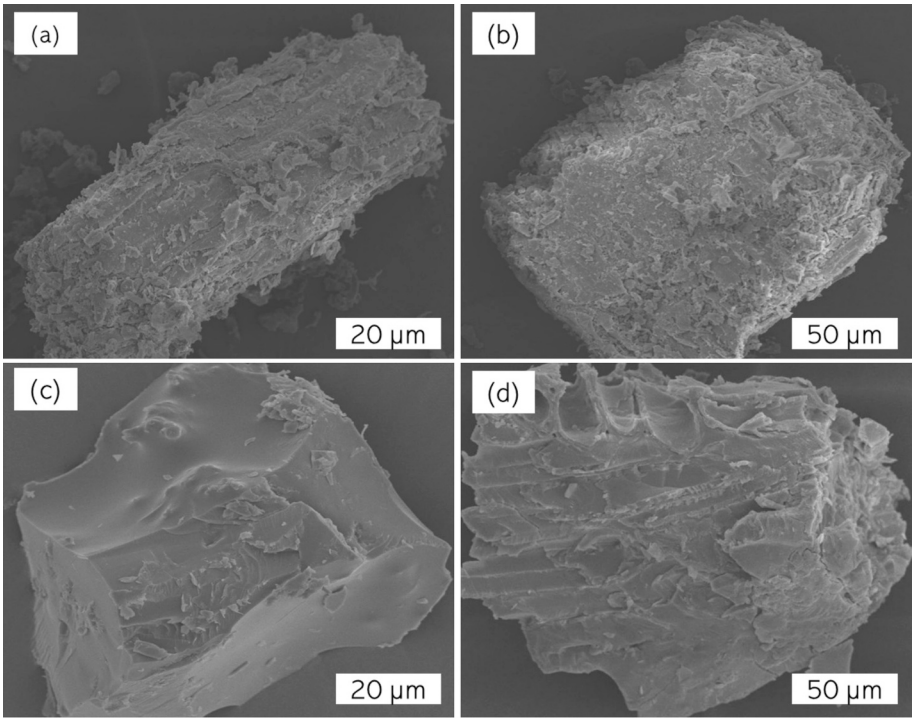

Fig. 2. SEM Images (a-b) of Raw Ghaf Waste and (c-d) Extracted Lignin.

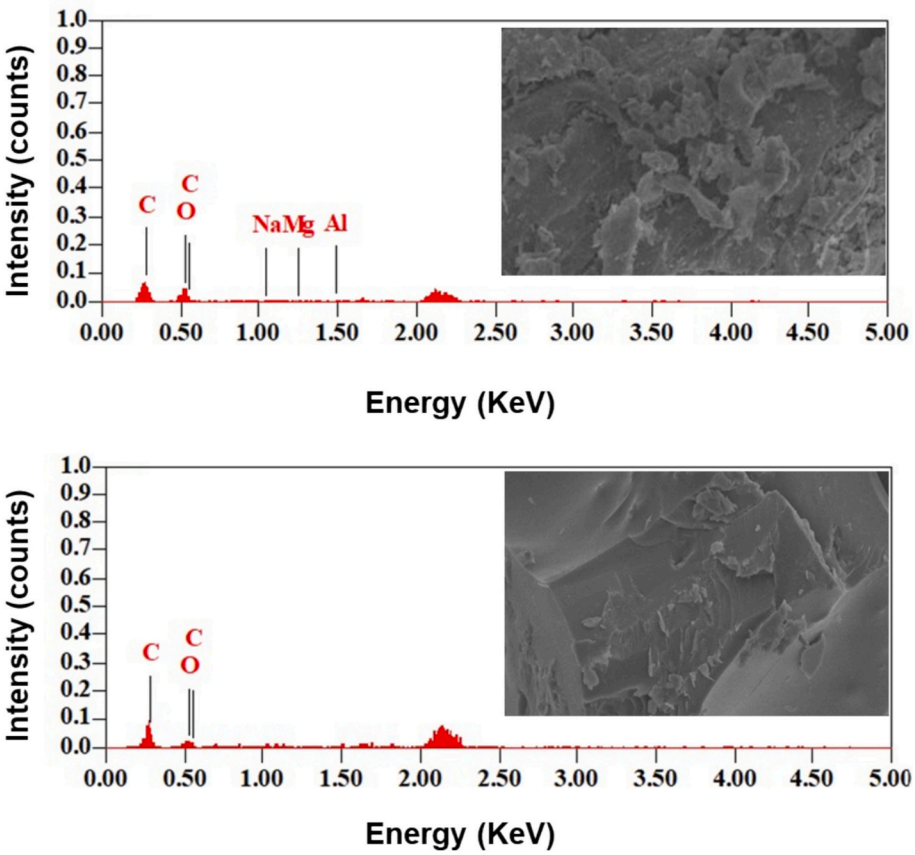

Fig. 3. Energy Dispersive X-ray (EDX) analysis of (a)- Raw Ghaf Waste and (b)- Extracted Lignin.

Table 3
Elemental composition of Raw Ghaf waste and Extracted Lignin.

Elements	Mass%		Atom%	
	Raw Ghaf	*Extracted Lignin*	*Raw Ghaf*	*Extracted Lignin*
C	63.15 ± 2.02	69.73 ± 0.54	69.90 ± 2.08	75.42 ± 0.47
O	35.10 ± 3.19	30.28 ± 0.54	29.17 ± 2.71	24.58 ± 0.47
C/O	1.80 ± 0.17	2.30 ± 0.05	2.40 ± 0.23	3.07 ± 0.06

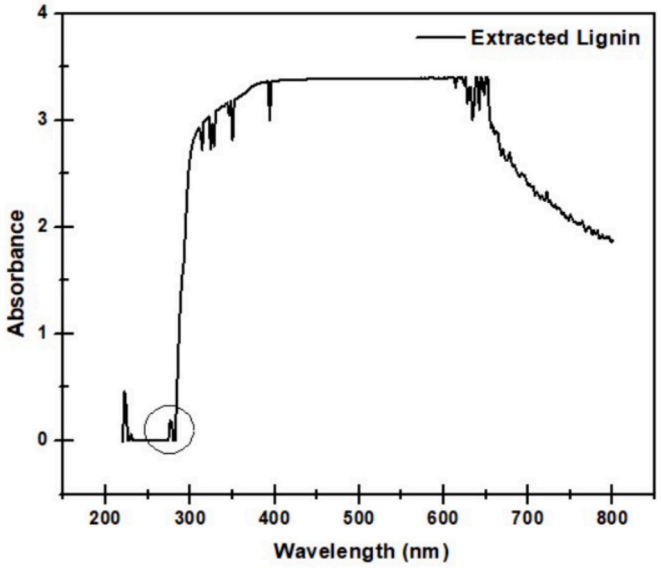

Fig. 4. UV–Vis absorbance spectra of extracted lignin.

[51].

3.5. XRD analysis

Fig. 5 presents the XRD diffractograms of the raw Ghaf waste and the extracted lignin. Raw Ghaf waste exhibited distinct peaks at 2θ = 15.35°, 22.60°, and 34.50°, which correspond to the crystallographic planes of cellulose Iβ, the prevalent polymorph in higher plants. These peaks are characteristic of lignocellulosic biomass and indicate the presence of crystalline cellulose structures [52]. Additionally, the peak at 2θ = 24.69° suggests a secondary reflection associated with cellulose Iβ, potentially signifying subtle crystalline rearrangements. This secondary peak may also be indicative of lignin–carbohydrate complexes (LCCs), where lignin forms ordered aggregates with polysaccharides, contributing to the overall crystalline structure of the biomass. The degree of crystallinity of the fibers can be assessed by analyzing the sharpness of the diffraction peaks, with sharper peaks indicating higher crystallinity [53]. An obvious reduction in the peak intensity was observed in the XRD spectra of the extracted lignin, signifying the effective removal of polysaccharides. Table 4 shows the XRD data for raw Ghaf waste and extracted lignin, showing the intensities of the amorphous (I_{am}) and crystalline (I_{200}) regions along with the corresponding crystallinity index (C_{rl}). For raw Ghaf waste, a C_{rl} of 41.46 % highlighted the significant presence of crystalline cellulose. After extraction, the C_{rl} of lignin decreased to 10.56 %, indicating a marked reduction in the crystalline content. This sharp decline reflects the effective removal of polysaccharides, primarily cellulose and hemicellulose, which are responsible for the crystalline regions of lignocellulosic

Table 4
X-ray diffraction analysis of Raw Ghaf Waste and Extracted Lignin.

Sample	Amorphous		Crystalline		C_{rl} (%)
	2θ	I_{am}	2θ	I_{200}	
Raw Ghaf	18.6	562.79	22.6	961.37	41.46
Extracted lignin	18.6	663.42	22.8	741.76	10.56

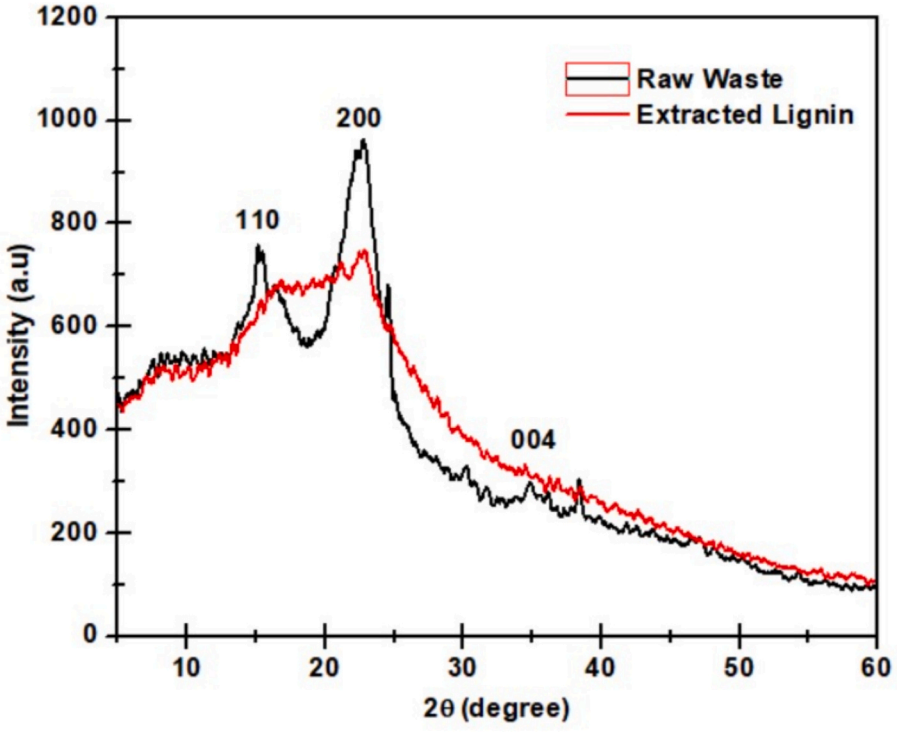

Fig. 5. XRD diffractograms of Raw Ghaf Waste and Extracted Lignin.

materials [38]. XRD analysis confirmed the effectiveness of this two-step lignin extraction and non-precipitation method in successfully removing crystalline parts (cellulose and hemicellulose) from lignocellulosic waste.

3.6. FTIR analysis

Fig. 6 shows the FTIR spectra of the raw Ghaf waste and extracted lignin. FTIR analysis identifies specific functional groups in a material by detecting their characteristic absorption bands, thereby effectively creating a molecular fingerprint [54]. The FTIR spectra of raw Ghaf waste and extracted lignin revealed significant changes, indicating a reduction in polysaccharides (cellulose and hemicellulose) and enrichment of lignin. In the raw Ghaf waste, prominent peaks associated with polysaccharides, such as C–O–C stretching in β-glycosidic linkages (~1148 cm^{-1}, 1023 cm^{-1}, 905 cm^{-1}), and C—H deformation vibrations from cellulose (~1375 cm^{-1} and 1316 cm^{-1}) were observed [55–57]. These peaks were significantly reduced or vanished in the extracted lignin spectrum, indicating that the polysaccharides were largely removed. Additionally, the broad O—H stretching band at 3414 cm^{-1}, typical of cellulose and hemicellulose, became sharper in the extracted lignin, reflecting the removal of polysaccharide hydroxyl groups and the presence of phenolic O—H groups. The peaks associated with aromatic ring vibrations (1617 cm^{-1}, 1507 cm^{-1}) are more noticeable in the extracted lignin, confirming the enrichment of lignin after treatment [37]. The significant reduction in the C═O stretching band at 1742 cm^{-1}, attributed to hemicellulose, further confirms the removal of hemicellulose [58]. FTIR analysis confirmed the effectiveness of this two-step lignin extraction and non-precipitation method in successfully removing the crystalline parts (cellulose and hemicellulose) and enriching lignin.

3.7. Thermogravimetric analysis (TGA)

Fig. 7 shows the TGA profiles of the raw Ghaf waste and extracted lignin. The curves exhibit the typical characteristics of lignocellulosic materials, with the decomposition process divided into three regions: dehydration, devolatilization (or main decomposition), and carbonization [59]. In lignocellulosic materials, the dehydration phase involves the release of moisture and light hydrocarbons. The main decomposition phase also referred to as the active pyrolysis region, corresponds to the breakdown of cellulose and hemicellulose into vapor-phase products, which later condense to form bio-oil. The carbonization phase involves the thermal degradation of lignin, resulting in the formation of a carbon-rich solid residue known as biochar [60]. The main decomposition region is particularly important for assessing the quantity of polysaccharides (cellulose and hemicellulose) in the material [61]. Hemicellulose typically decomposes between 180 and 300 °C, cellulose between 300 and 400 °C, and lignin over a broader range of 300–500 °C because of its complex aromatic structure [62]. Table 5 shows the thermal decomposition characteristics of the raw Ghaf waste and extracted lignin. In the raw Ghaf waste, the onset temperature (T_{onset}) is observed at 238 °C, with an initial 8.72 % mass loss. The devolatilization range (238–364 °C), which mainly corresponds to the decomposition of cellulose and hemicellulose, exhibited a 54.06 % mass loss, reflecting the significant presence of these polysaccharides. In contrast, the extracted lignin begins to decompose earlier, with a T_{onset} of 202 °C, due to the removal of cellulose, which is a highly stable biopolymer, with an initial 7.01 % mass loss, while the devolatilization range (202–362 °C) shows only 30.77 % mass loss. The mass loss in the devolatilization region was reduced by 43.08 % in the extracted lignin compared to that in the raw Ghaf waste. This was due to the absence of cellulose and hemicellulose in the extracted lignin. The higher char residue (36.92 %) at 700 °C in the extracted lignin compared to 20.85 % in raw Ghaf waste indicates the presence of more carbon-rich material, primarily lignin, which is more thermally stable. The reduced mass loss in the devolatilization region, combined with the increased char yield, indicates the enriched aromatic nature of the extracted lignin. Mohsin et al. [38] performed the TGA of raw date fruit seeds at a heating rate of 20 °C/min. The main decomposition range consisted of 205–330 °C with a mass loss

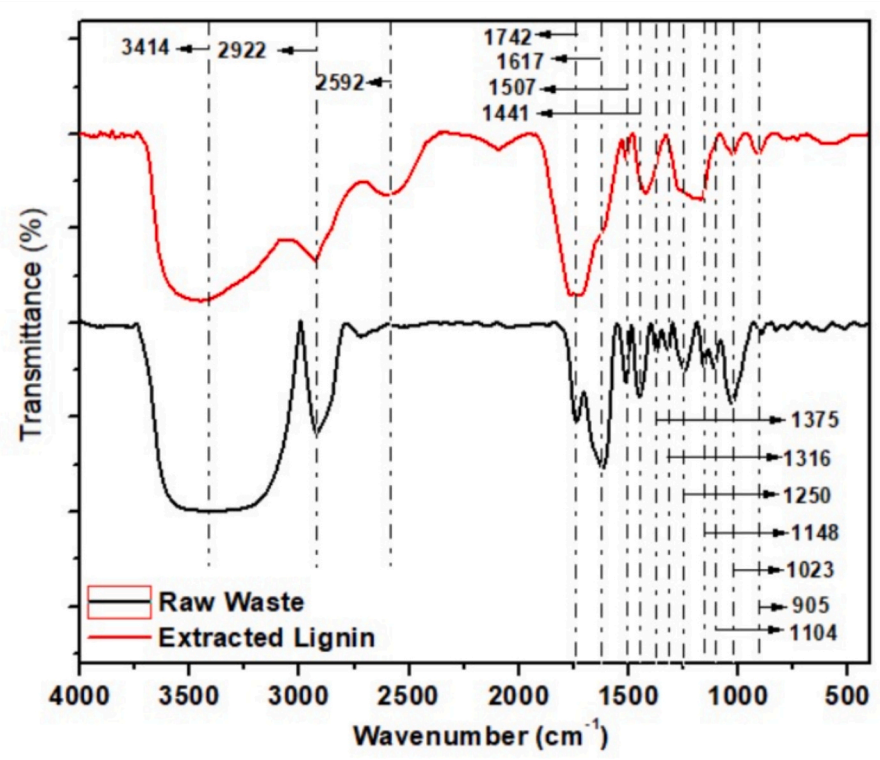

Fig. 6. FTIR spectra of Raw Ghaf Waste and Extracted Lignin.

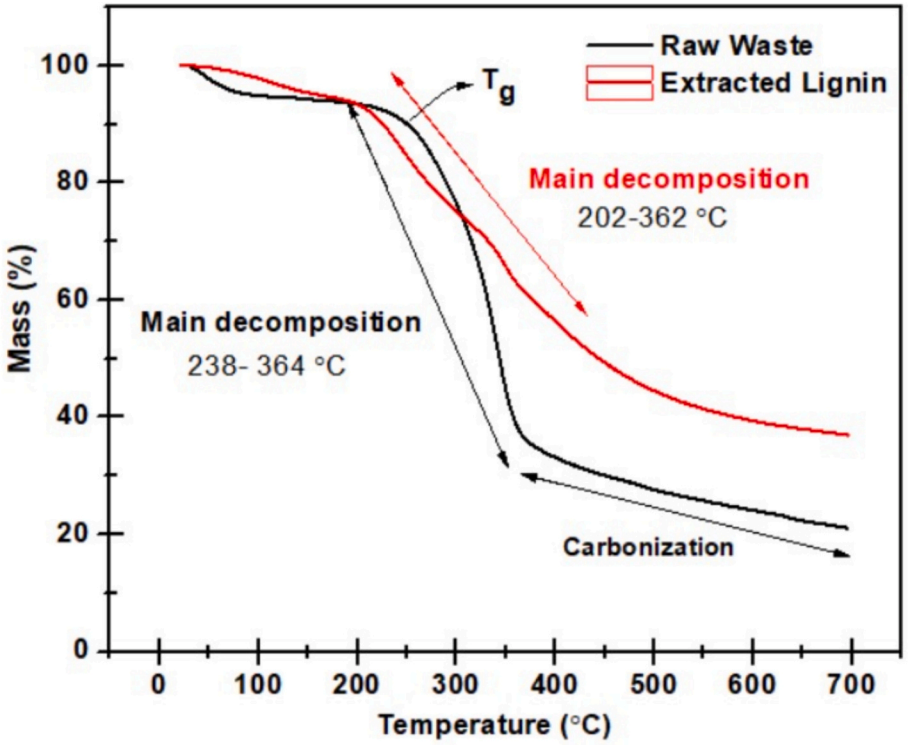

Fig. 7. TGA profiles of Raw Ghaf Waste and Extracted Lignin.

Table 5
Thermal characteristic properties of Raw Ghaf Waste and Extracted Lignin.

Material	T_{onset} (°C)	$Mass_{loss}$ (%) at T_{onset}	Devolatilization range (°C)	$Mass_{loss}$ (%) in the Devolatilization range	Char (%)
Raw Ghaf	238	8.72	238–364	54.06	20.85
Extracted Lignin	202	7.01	202–362	30.77	36.92

of 50.27 % in the devolatilization region. Ilyas et al. [53] performed the TGA of raw sugar palm fibers at a heating rate of 10 °C/min. The main decomposition range consisted of 210–345 °C with a mass loss of 43.76 % in the devolatilization region. Raza et al. performed the TGA of cashew shell waste at a heating rate of 10 °C/min. The main decomposition range consisted of 253–372 °C with a mass loss of 68.70 % in the devolatilization region.

Fig. 8 shows the differential thermogravimetric (DTG) curves of the raw Ghaf waste and extracted lignin. In the raw Ghaf waste, peaks at 275 °C, 340 °C, and 492 °C corresponded to the degradation of hemicellulose, cellulose, and lignin, respectively. Hemicellulose decomposes first because of its lower thermal stability, followed by a sharp cellulose peak at 340 °C, indicating the primary breakdown of its crystalline regions. Lignin in the raw biomass degrades gradually, with a broader peak at 492 °C, reflecting its complex structure and resistance to thermal degradation. For the extracted lignin, peaks were observed at 244 °C, 349 °C, and 411 °C. The 244 °C peak suggests the breakdown of low molecular weight compounds or residual impurities. The prominent 349 °C and 411 °C peaks correspond to the primary and secondary decomposition of lignin, involving cleavage of ether bonds and degradation of aromatic units. Additionally, the decomposition behavior of the extracted lignin in this study is comparable to that of commercial lignin, as reported by [29], who observed DTG peaks at 245 °C, 418 °C, and 590 °C. This similarity confirms that the lignin extracted from the Ghaf waste follows a typical lignin decomposition pattern, validating its high purity. Furthermore, the absence of 275 °C and 340 °C peaks in the lignin curve confirmed the successful removal of hemicellulose and cellulose. Both TGA and DTG analyses confirmed the effectiveness of this two-step lignin extraction and non-precipitation method in successfully removing the crystalline parts (cellulose and hemicellulose) and enriching lignin.

3.8. Diffraction Scanning Calorimetry (DSC)

Fig. 9 shows the DSC thermograph of the extracted lignin, which reveals two distinct endothermic peaks. The first peak at 155 °C corresponds to moisture loss or the evaporation of residual volatiles from the NADES extraction process, whereas the second, more pronounced peak at 201 °C indicates the onset of thermal softening, bond rearrangements, or early decomposition. Beyond 201 °C, the curve stabilized, presenting no significant thermal transitions up to the measured range of 300 °C. The thermal transition behavior of the extracted lignin in this study closely aligns with that of commercial lignin reported by Meraj et al. [29], who observed peaks at 132 °C and 169.25 °C, and by Yan et al. [63], who identified closely related peaks for Kraft lignin at 146.5 °C and 219.7 °C. These findings confirm that 100 % organic NADES-extracted lignin exhibits thermal transition characteristics comparable to those of commercial lignin.

3.9. Activation energy (E_a) analysis

Table 6 shows the E_a values for raw Ghaf waste and extracted lignin at different degrees of conversion (α) using three kinetic models: Flynn-Wall-Ozawa (FWO), Kissinger-Akahira-Sunose (KAS), and Starink (STK). For raw Ghaf waste, the E_a value is relatively low (15–43 kJ/mol) at lower α, which increases significantly at intermediate values of α

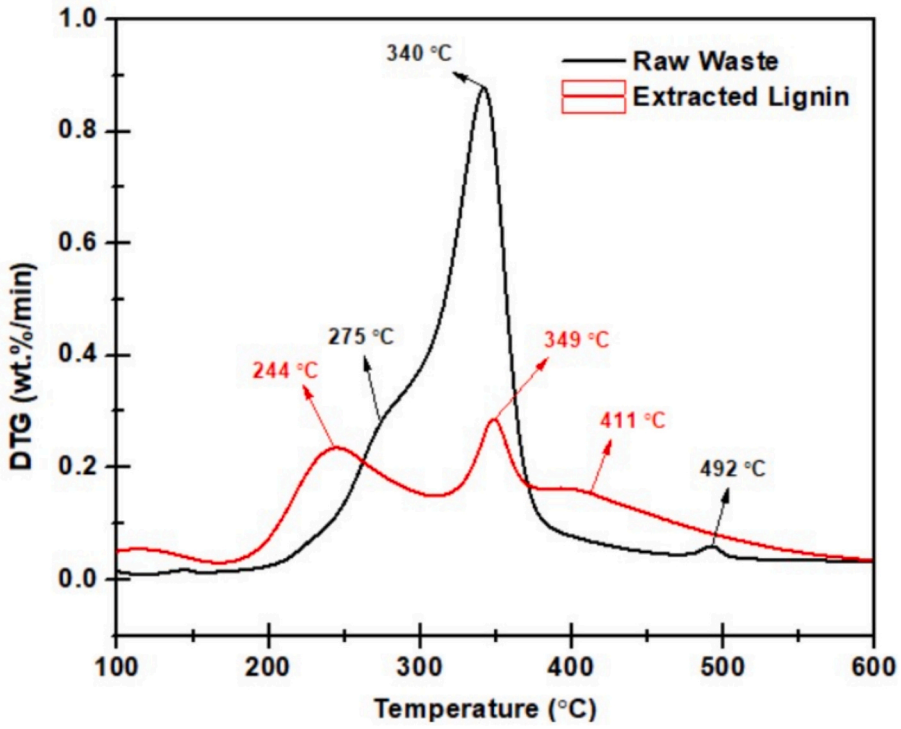

Fig. 8. DTG profiles of Raw Ghaf Waste and Extracted Lignin.

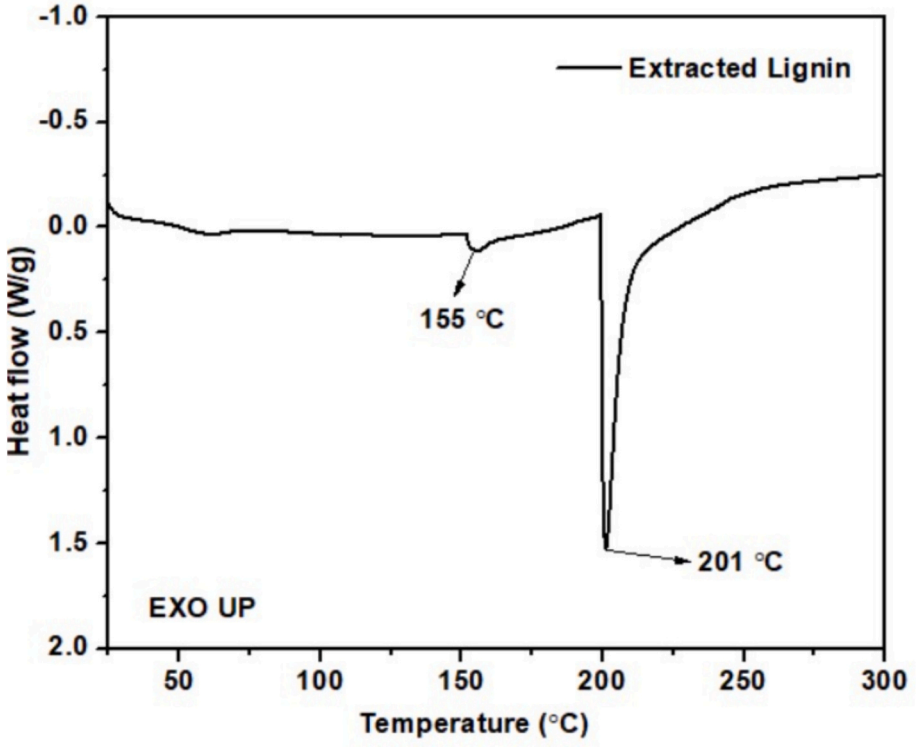

Fig. 9. DSC thermogram for extracted lignin.

(117–158 kJ/mol) due to the decomposition of cellulose and fluctuates further at higher α values, probably due to residual lignin and char formation. In contrast, the extracted lignin showed consistently higher E_a values (22–140 kJ/mol), starting with moderate α values and peaking at medium values (158–254 kJ/mol), because of the degradation of its complex aromatic structure. The average E_a values confirmed the higher thermal stability of lignin (E_a≈155 kJ/mol) than that of raw Ghaf waste (E_a=131 kJ/mol). Because lignin has a complex structure consisting of highly cross-linked aromatic rings, it requires a higher E_a for thermal degradation. This 24 % higher E_a of extracted lignin compared to E_a of

Table 6
E_a (kJ/mol) of Raw Ghaf Waste and Extracted Lignin.

Conversion (α)	E_a (kJ/mol)-Raw Waste			E_a (kJ/mol)-Extracted Lignin		
	FWO	KAS	STK	FWO	KAS	STK
0.05	15.34	22.25	21.98	22.39	17.10	17.34
0.10	43.55	54.20	53.82	114.73	112.68	112.91
0.15	41.77	34.93	35.26	140.78	139.68	139.90
0.20	120.77	117.78	118.06	158.24	157.69	157.91
0.25	116.58	113.15	113.43	171.95	171.63	171.87
0.30	119.23	115.74	116.04	175.14	174.41	174.66
0.35	135.62	132.84	133.13	254.07	256.99	257.20
0.40	158.47	156.77	157.04	238.13	239.82	240.05
0.45	182.67	182.13	182.38	222.95	223.38	223.65
0.50	200.62	200.92	201.16	100.04	117.09	116.53
0.55	205.46	205.90	206.14	232.74	232.38	232.69
0.60	192.14	191.70	191.96	16.25	30.73	30.16
0.65	250.83	252.95	253.18	–	–	–
0.70	146.30	165.67	165.07	–	–	–
0.75	29.63	44.09	43.54	–	–	–
Avg.	130.60	132.73	132.81	153.95	156.13	156.24

raw Ghaf waste is a sign of lignin's resistance to thermal degradation and underlines its potential for use in high-temperature processes. These values provide important insights for the optimization of thermochemical processes, such as pyrolysis and gasification, to convert lignin into value-added products, such as bio-oil, biochar, and phenolic compounds. Table 7 lists the E_a values for various lignocellulosic biomasses and lignins. Raw Ghaf waste exhibits a moderate E_a of 131 kJ/mol, whereas other biomasses such as date palm fiber (E_a=113–114 kJ/mol) and cashew waste (E_a=130–174 kJ/mol) exhibit lower to moderate thermal stability. In contrast, denser and lignin-rich materials, such as pine wood (E_a=218 kJ/mol) and mustard straw (E_a=200–205 kJ/mol), exhibit significantly higher $E_a$values, indicating greater resistance to thermal degradation. The extracted lignin generally exhibits higher thermal stability than raw Ghaf biomass because of its complex aromatic and cross-linked structure, with $E_a$values ranging from 155 kJ/mol in this study to 180 kJ/mol in other studies. Enzymatic lignin, however, has a lower E_a of 110 kJ/mol, which is probably due to structural changes during the extraction process. Lignin's higher E_a makes it suitable for high-temperature applications, such as biochar production, while biomasses with lower E_a are more suitable for bio-oil and syngas production. E_a values are important for the optimization of pyrolysis and gasification processes for the efficient conversion of biomass and lignin into valuable bio-based products.

Table 7
E_a (kJ/mol) for different lignocellulose biomasses and lignin.

Biomass	E_a (kJ/mol)	Model	Ref.
Lignocellulose Waste			
Raw Ghaf Waste	131	Model free-FWO, KAS, STK	This study
Date Palm Surface Fibers	113–114	Model fitting-Coats-Redfern	[64]
Cashew Waste	130–174	Model fitting-Coats-Redfern	[65]
Pine Wood	218	Model fitting-Coats-Redfern	[66]
Sawdust	170–210	Model free-FWO, KAS, Friedman, and DAEM	[67]
Mustard straw	200–205	Model free- FWO, KAS, and Vyazovkin	[68]
Lignin			
Extracted lignin	155	Model free-FWO, KAS, STK	This study
Lignin	180	Model free-DAEM	[69]
Alkaline lignin	158.94	Model free-FWO, KAS	[70]
Enzymatic lignin	110	Two-step reaction model	[71]

Table 8
Ultimate analysis of Raw Ghaf Waste and Extracted Lignin.

Ultimate analysis (%)	Raw Ghaf Waste	Extracted Lignin
Carbon (C)	44.62 ± 0.22	53.22 ± 0.24
Hydrogen (H)	3.34 ± 0.13	2.10 ± 0.08
Nitrogen (N)	0.91 ± 0.0	0.136 ± 0.0
Sulfur (S)	0.061 ± 0.01	0.042 ± 0.01
Oxygen (O)	51.06 ± 0.33	44.49 ± 0.27

3.10. Elemental analysis

Table 8 shows the ultimate analysis of the raw Ghaf waste and extracted lignin and provides information on the elemental composition in terms of carbon (C), hydrogen (H), nitrogen (N), sulfur (S), and oxygen (O). The analysis showed that the extracted lignin had a significantly higher carbon content (53.22 ± 0.24 %) than raw Ghaf waste (44.62 ± 0.22 %), indicating a successful fractionation process that increases the purity of the lignin. The hydrogen content decreased from 3.34 ± 0.13 % to 2.10 ± 0.08 %, indicating the removal of polysaccharides, which typically have a higher hydrogen content. In addition, the nitrogen and sulfur contents are reduced due to the removal of protein and sulfur-containing compounds, making the extracted lignin more environmentally friendly for thermal applications. The oxygen content decreased from 51.06 ± 0.33 % to 44.49 ± 0.27 %, which was consistent with the selective removal of oxygen-rich carbohydrates and extractives. This change in composition improved the thermal stability and carbon content of the extracted lignin, making it a promising candidate for biodegradable composites, bio-based carbon materials, and energy-efficient insulation applications.

4. Conclusion

This study presents a novel and environmentally friendly approach to lignin extraction using NADES consisting of citric acid and fructose. This innovative acid-free process for lignin extraction eliminates the need for conventional acid precipitation and is, therefore, in line with the principles of green chemistry. Extraction using NADES resulted in a maximum lignin yield of 9.50 % and a recovery rate of 44.10 %. Characterization confirmed high-purity lignin with preserved aromatic structures, improved thermal stability, and increased carbon content. The SEM, FTIR, XRD, UV–Vis, and thermal analyses using TGA and DSC confirmed the effectiveness of this method. This study sets a sustainable standard for the valorization of lignin and promotes environmentally friendly biorefinery practices and circular economic strategies for biomass utilization. Future research studies can focus on the scale-up of the extraction process. Moreover, solvent recovery and reusability, together with techno-economic analysis, bring further addition to this area of research. The utilization of extracted lignin for value-added products such as to make bio-urethane and compare the performance with conventional materials.

CRediT authorship contribution statement

Mohsin Raza: Writing – original draft, Methodology, Investigation, Formal analysis, Data curation, Conceptualization. **Arafat Husain:** Writing – review & editing, Methodology, Formal analysis, Data curation, Conceptualization. **Mohammad Jawaid:** Writing – review & editing, Methodology, Formal analysis, Data curation, Conceptualization. **Abrar Inayat:** Writing – review & editing, Formal analysis, Data curation. **Yaser E. Greish:** Writing – review & editing, Formal analysis, Data curation. **Aatikah Meraj:** Formal analysis, Data curation. **Basim Abu-Jdayil:** Writing – review & editing, Supervision, Resources, Methodology, Investigation, Funding acquisition, Formal analysis, Data curation, Conceptualization.

Consent for publication

All authors agreed to publish the research findings.

Funding

This research was funded by a research grant from the United Arab Emirates University [grant number: 12R211 and 12R294].

Declaration of competing interest

The authors declare the following financial interests/personal relationships which may be considered as potential competing interests: Prof. Basim Abu-Jdayil reports financial support was provided by United Arab Emirates University. If there are other authors, they declare that they have no known competing financial interests or personal relationships that could have appeared to influence the work reported in this paper.

Acknowledgments

All the authors are grateful to the Department of Chemical and Petroleum Engineering at the United Arab Emirates University, UAE.

References

[1] S.S. Patil, U. Sharma, Implementing sustainable methods in natural products research, in: Trends in Chemistry, 2024.
[2] I. Alawad, H. Ibrahim, Pretreatment of agricultural lignocellulosic biomass for fermentable sugar: opportunities, challenges, and future trends, Biomass Convers. Biorefinery 14 (5) (2024) 6155–6183.
[3] T. Rashid, et al., Enhanced lignin extraction and optimisation from oil palm biomass using neural network modelling, Fuel 293 (2021) 120485.
[4] J. Kim, et al., Advancing biomass fractionation with real-time prediction of lignin content and MWd: A kMC-based multiscale model for optimized lignin extraction, Chem. Eng. J. 479 (2024) 147226.
[5] S. Shah, et al., Lignin-based additive materials: A review of current status, challenges, and future perspectives, Addit. Manuf. 74 (10) (2023) 1016.
[6] H.A. Ariyanta, et al., Current roles of lignin for the agroindustry: Applications, challenges, and opportunities, Int. J. Biol. Macromol. 240 (2023) 124523.
[7] I. Othman, et al., Extraction of crystalline nanocellulose from palm tree date seeds (Phoenix dactylifera L.), Chem. Eng. Commun. 210 (1) (2023) 61–73.
[8] M. Raza, L. Ali, M. Altarawneh, B. Abu-Jdayil, Evaluation of thermal pyrolysis characteristics and kinetic parameters of cellulose extracted from date waste using natural deep eutectic solvent, Case Studies in Chemical and Environmental Engineering 10 (2024) 100796.
[9] M. Gallego-García, A.D. Moreno, P. Manzanares, M.J. Negro, A. Duque, Recent advances on physical technologies for the pretreatment of food waste and lignocellulosic residues, Bioresour. Technol. 369 (2023) 128397.
[10] E.J. Panakkal, et al., A comparative study on effectiveness and recyclability of three different deep eutectic solvents for biomass fractionation, Biomass Convers. Biorefinery (2024) 1–15.
[11] A. Meraj, S.P. Singh, M. Jawaid, M.M. Nasef, T.S. Alomar, N. AlMasoud, A review on eco-friendly isolation of lignin by natural deep eutectic solvents from agricultural wastes, J. Polym. Environ. 31 (8) (2023) 3283–3316.
[12] S. Hilali, et al., NaDES-based biorefinery of Spirulina (Arthrospira platensis): A new path for sustainable high value-added metabolites, Sep. Purif. Technol. 329 (2024) 125123.
[13] M.S. Che Zain, J.X. Yeoh, S.Y. Lee, K. Shaari, Physicochemical properties of choline chloride-based natural deep eutectic solvents (Nades) and their applicability for extracting oil palm flavonoids, Sustainability 13 (23) (2021) 12981.
[14] Q. Ji, L. Su, Z. Li, I.D. Boateng, X. Liu, Preparation of peanut shell lignin nanocellulose by aluminum trichloride acid deep eutectic solvent pretreatment, Biomass Convers. Biorefinery (2025) 1–22.
[15] Z. Chen, A. Ragauskas, C. Wan, Lignin extraction and upgrading using deep eutectic solvents, Ind. Crop. Prod. 147 (2020) 112241.
[16] T. Xiao, et al., Recent progress in deep eutectic solvent (DES) fractionation of lignocellulosic components: A review, Renew. Sust. Energ. Rev. 192 (2024) 114243.
[17] M.A. Alam, et al., Choline chloride-based deep eutectic solvents as green extractants for the isolation of phenolic compounds from biomass, J. Clean. Prod. 309 (2021) 127445.
[18] C. Sitthisak, et al., Efficient extraction of quassinoids and alkaloids from Eurycoma longifolia Jack roots using natural deep eutectic solvents and microwave-assisted extraction, Microchem. J. 196 (2024) 109676.
[19] A. Kaleta, et al., The Effects of selected extraction methods and natural deep eutectic solvents on the recovery of active principles from *Aralia elata* var. mandshurica (Rupr. & Maxim.) J. Wen: A non-targeted metabolomics approach, Pharmaceuticals 17 (3) (2024), p. 355.
[20] J. Yao, et al., Effect of deep eutectic solvent extraction on Auricularia auricula polysaccharide solubilization and antioxidant potential, Sustain. Chem. Pharm. 34 (2023) 101166.
[21] A.N. Shikov, V.M. Kosman, E.V. Flissyuk, I.E. Smekhova, A. Elameen, O. N. Pozharitskaya, Natural deep eutectic solvents for the extraction of phenyletanes and phenylpropanoids of Rhodiola rosea L, Molecules 25 (8) (2020) 1826.
[22] V. Huber, L. Muller, P. Degot, D. Touraud, W. Kunz, NADES-based surfactant-free microemulsions for solubilization and extraction of curcumin from Curcuma Longa, Food Chem. 355 (2021) 129624.
[23] P.S. Suresh, P.P. Singh, M. Sharma, U. Sharma, Multicomponent natural deep eutectic solvents: Super solvents for the efficient extraction of steviol glycosides (rebaudioside A) from Stevia rebaudiana, J. Clean. Prod. 385 (2023) 135639.
[24] G. Aggarwal, P.P. Singh, M.K. Gupta, U. Sharma, NADES-based essential oil extraction and isolation of new epoxysesquiterpene from Ageratina adenophora flowers, J. Mol. Struct. 1292 (2023) 136077.
[25] K. Parmar, G. Aggarwal, U. Sharma, α-Glucosidase Inhibiting Chromene Derivatives from Ageratum conyzoides L. Essential Oil Extracted via NADES-Assisted Hydrodistillation, Chem. Biodivers. 22 (1) (2025) e202401324.
[26] P.S. Suresh, P.P. Singh, S. Kapoor, Y.S. Padwad, U. Sharma, Lactic acid-based deep eutectic solvent: An efficient green media for the selective extraction of steroidal saponins from Trillium govanianum, Sep. Purif. Technol. 294 (2022) 121105.
[27] P.P. Singh, Anmol, P.S. Suresh, U. Sharma, NADES extraction, UHPLC-ELSD-based quantification, and network pharmacology-guided target identification of fourteen specialised metabolites from Trillium govanianum Wall. ex D. Don, Phytochem. Anal. 35 (6) (2024) 1265–1277.
[28] I.F. Mota, J. da Silva Burgal, F. Antunes, M.E. Pintado, P.S. Costa, High value-added lignin extracts from sugarcane by-products, Int. J. Biol. Macromol. 230 (2023) 123144.
[29] A. Meraj, et al., Isolation and characterisation of lignin using natural deep eutectic solvents pretreated kenaf fibre biomass, Sci. Rep. 14 (1) (2024) 8672.
[30] M. Raza, M. Jawaid, B. Abu-Jdayil, Enhanced nanocellulose extraction from date palm waste: green solvent hydrolysis with transition metal complex, Sci. Rep. 14 (1) (2024) 21960.
[31] M. Sharma, J. Marques, A. Simões, M.M. Donato, O. Cardoso, L.M. Gando-Ferreira, Optimization of lignin precipitation from black liquor using organic acids and its valorization by preparing lignin nanoparticles, Int. J. Biol. Macromol. 269 (2024) 131881.
[32] D. Gallacher, J. Hill, Status of Prosopis cineraria (ghaf) tree clusters in the Dubai Desert Conservation Reserve, Tribulus 15 (2) (2005).
[33] W. Al Yamani, et al., Water use of Al Ghaf (Prosopis cineraria) and Al Sidr (Ziziphus spina-christi) forests irrigated with saline groundwater in the hyper-arid deserts of Abu Dhabi, Agric. Water Manag. 203 (2018) 105–114.
[34] O.N. Pozharitskaya, et al., Physicochemical and Antimicrobial Properties of Lactic Acid-Based Natural Deep Eutectic Solvents as a Function of Water Content, Appl. Sci. 14 (22) (2024) 2076–3417.
[35] Y. Liu, et al., Tunable and functional deep eutectic solvents for lignocellulose valorization, Nat. Commun. 12 (1) (2021) 5424.
[36] L. Soto-Salcido, I. Anugwom, L. Ballinas-Casarrubias, M. Mänttäri, M. Kallioinen, NADES-based fractionation of biomass to produce raw material for the preparation of cellulose acetates, Cellulose 27 (2020) 6831–6848.
[37] M. Raza, B. Abu-Jdayil, F. Banat, A.H. Al-Marzouqi, Isolation and characterization of cellulose nanocrystals from date palm waste, ACS Omega 7 (29) (2022) 25366–25379.
[38] M. Raza, B. Abu-Jdayil, Extraction of cellulose nanocrystals from date seeds using transition metal complex-assisted hydrochloric acid hydrolysis, Int. J. Biol. Macromol. 294 (2025) 139477.
[39] L. Segal, J.J. Creely, A. Martin Jr., C. Conrad, An empirical method for estimating the degree of crystallinity of native cellulose using the X-ray diffractometer, Text. Res. J. 29 (10) (1959) 786–794.
[40] J. Fu, et al., Co-circularity of spent coffee grounds and polyethylene via co-pyrolysis: characteristics, kinetics, and products, Fuel 337 (2023) 127061.
[41] Y. Wang, S. Yang, G. Bao, H. Wang, Investigation of tobacco straw pyrolysis: Three-parallel Gaussian reaction modeling, products analysis and ANN application, Ind. Crop. Prod. 200 (2023) 116864.
[42] C. Ma, F. Zhang, J. Hu, H. Wang, S. Yang, H. Liu, Co-pyrolysis of sewage sludge and waste tobacco stem: Gas products analysis, pyrolysis kinetics, artificial neural network modeling, and synergistic effects, Bioresour. Technol. 389 (2023) 129816.
[43] E.O. Owhe, N. Kumar, J.G. Lynam, Lignin extraction from waste biomass with deep eutectic solvents: molecular weight and heating value, Biocatal. Agric. Biotechnol. 32 (2021) 101949.
[44] J.G. Lynam, N. Kumar, M.J. Wong, Deep eutectic solvents' ability to solubilize lignin, cellulose, and hemicellulose; thermal stability; and density, Bioresour. Technol. 238 (2017) 684–689.
[45] V. Provost, S. Dumarcay, I. Ziegler-Devin, M. Boltoeva, D. Trébouet, M. Villain-Gambier, Deep eutectic solvent pretreatment of biomass: Influence of hydrogen bond donor and temperature on lignin extraction with high β-O-4 content, Bioresour. Technol. 349 (2022) 126837.
[46] J. Zhu, L. Xue, W. Wei, C. Mu, M. Jiang, Z. Zhou, Modification of lignin with silane coupling agent to improve the interface of poly (L-lactic) acid/lignin composites, BioResources 10 (3) (2015) 4315–4325.
[47] M. Raza, M. Jawaid, B. Abu-Jdayil, Nanocellulose extraction from date palm waste using 1-butyl-3-methylimidazolium hydrogen sulphate, Int. J. Biol. Macromol. 249 (2025) 139539.

[48] J. Intapun, T. Rungruang, S. Suchat, B. Cherdchim, S. Hiziroglu, The Characteristics of natural rubber composites with Klason lignin as a green reinforcing filler: Thermal stability, mechanical and dynamical Properties, Polymers 13 (7) (2021) 1109.
[49] N. Smyk, J. Sjöström, G. Henriksson, O. Sevastyanova, UV–vis spectroscopy as a rapid method for evaluation of total phenolic hydroxyl structures in lignin, Nord. Pulp Pap. Res. J. 39 (4) (2024) 731–746.
[50] O. Morozova, et al., Green Extraction of Reed Lignin: The Effect of the Deep Eutectic Solvent Composition on the UV-Shielding and Antioxidant Properties of Lignin, Int. J. Mol. Sci. 25 (15) (2024) 8277.
[51] D.R. Lobato-Peralta, et al., A review on trends in lignin extraction and valorization of lignocellulosic biomass for energy applications, J. Clean. Prod. 293 (2021) 126123.
[52] L. Kian, N. Saba, M. Jawaid, O. Alothman, H. Fouad, Properties and characteristics of nanocrystalline cellulose isolated from olive fiber, Carbohydr. Polym. 241 (2020) 116423.
[53] R. Ilyas, S. Sapuan, M. Ishak, Isolation and characterization of nanocrystalline cellulose from sugar palm fibres (Arenga Pinnata), Carbohydr. Polym. 181 (2018) 1038–1051.
[54] Y. Huang, D.T. Sekyere, J. Zhang, Y. Tian, Fast pyrolysis behaviors of biomass with high contents of ash and nitrogen using TG-FTIR and Py-GC/MS, J. Anal. Appl. Pyrolysis 170 (2023) 105922.
[55] M.S. Islam, N. Kao, S.N. Bhattacharya, R. Gupta, H.J. Choi, Potential aspect of rice husk biomass in Australia for nanocrystalline cellulose production, Chin. J. Chem. Eng. 26 (3) (2018) 465–476.
[56] K.S. Prado, M.A. Spinacé, Isolation and characterization of cellulose nanocrystals from pineapple crown waste and their potential uses, Int. J. Biol. Macromol. 122 (2019) 410–416.
[57] Y. Guo, Y. Zhang, D. Zheng, M. Li, J. Yue, Isolation and characterization of nanocellulose crystals via acid hydrolysis from agricultural waste-tea stalk, Int. J. Biol. Macromol. 163 (2020) 927–933.
[58] M. Jawaid, L.K. Kian, H. Fouad, R. Khiari, O.Y. Alothman, M. Hashem, Cellulose Nanocrystal from Washingtonia Fibre and Its Characterization, J Renew Mater 10 (2022) 1459–1470.
[59] M. Raza, M. Jawaid, B. Abu-Jdayil, Extraction of lignin-containing nanocellulose fibrils from date palm waste using a green solvent, Int. J. Biol. Macromol. 267 (2024) 131540.
[60] M. Afraz, et al., Production of value added products from biomass waste by pyrolysis: An updated review, Waste Management Bulletin 1 (4) (2024) 30–40.
[61] V. Piazza, et al., Detailed speciation of biomass pyrolysis products with a novel TGA-based methodology: the case-study of cellulose, J. Anal. Appl. Pyrolysis 178 (2024) 106413.
[62] S. Zhang, Y. Mei, G. Lin, Pyrolysis interaction of cellulose, hemicellulose and lignin studied by TG-DSC-MS, J. Energy Inst. 112 (2024) 101479.
[63] Q. Yan, R. Arango, J. Li, Z. Cai, Fabrication and characterization of carbon foams using 100% Kraft lignin, Mater. Des. 201 (2021) 109460.
[64] M. Raza, B. Abu-Jdayil, A.H. Al-Marzouqi, A. Inayat, Kinetic and thermodynamic analyses of date palm surface fibers pyrolysis using Coats-Redfern method, Renew. Energy 183 (2022) 67–77.
[65] A.J. Tsamba, W. Yang, W. Blasiak, Pyrolysis characteristics and global kinetics of coconut and cashew nut shells, Fuel Process. Technol. 87 (6) (2006) 523–530.
[66] I. Mian, et al., Kinetic study of biomass pellet pyrolysis by using distributed activation energy model and Coats Redfern methods and their comparison, Bioresour. Technol. 294 (2019) 122099.
[67] R.K. Mishra, K. Mohanty, Pyrolysis kinetics and thermal behavior of waste sawdust biomass using thermogravimetric analysis, Bioresour. Technol. 251 (2018) 63–74.
[68] A. Nawaz, P. Kumar, Pyrolysis of mustard straw: Evaluation of optimum process parameters, kinetic and thermodynamic study, Bioresour. Technol. 340 (2021) 125722.
[69] K.H. Kim, K. Jeong, S.-S. Kim, R.C. Brown, Kinetic understanding of the effect of Na and Mg on pyrolytic behavior of lignin using a distributed activation energy model and density functional theory modeling, Green Chem. 21 (5) (2019) 1099–1107.
[70] X. Liang, et al., Thermal kinetics of a lignin-based flame retardant, Polymers 12 (9) (2020) 2123.
[71] J. Cho, S. Chu, P.J. Dauenhauer, G.W. Huber, Kinetics and reaction chemistry for slow pyrolysis of enzymatic hydrolysis lignin and organosolv extracted lignin derived from maplewood, Green Chem. 14 (2) (2012) 428–439.